

Millimeter-wave Performance of Broadband Aperture Antenna on Laminates

Rashaunda Henderson, Richard Pierce,
Supreetha Aroor, Joel Arzola, Christopher Miller,
Harini Kumar, Thethnin Ei, Andrew Blanchard

Electrical Engineering Dept.
The University of Texas at Dallas
Richardson, TX, USA

Dave Fooshe, Bert Schluper,
Dan Swan, Carlos Morales

Nearfield Systems Inc.
Torrance, CA, USA

Abstract—This paper summarizes the design, fabrication and characterization of a coplanar waveguide fed modified aperture bowtie antenna operating in the 60 to 90 GHz range. Modifications to the bowtie edges extend the bandwidth up to 40% without increasing radiator area. The antenna was initially designed and measured in the 3-8 GHz frequency band and then frequency scaled to 60-90 GHz. The millimeter wave antenna is implemented on FR408 ($\epsilon_r=3.65$) and a multilayer laminate. Both substrates can be used in millimeter-wave system design where efficient antennas are needed. Return loss measurements of the antennas are made on a Cascade probe station. The results agree well with simulations in ANSYS HFSS. Until recently, only simulated radiation patterns were available illustrating broadside gain of 5 to 7 dB for these antennas. With the acquisition of a spherical scanner, near-field measurements have been taken of the three antennas from 67 to 110 GHz. The broadside radiation pattern results are compared with simulation. The NSI 700S-360 spherical near-field measurement system used in conjunction with an Agilent network analyzer, GGB Picoprobes and Cascade manipulator allow for on-wafer measurements of the antenna under test.

I. INTRODUCTION

Planar antennas are being designed in the 60-90 GHz range for use in several applications ranging from automotive radar to high-definition home video [1]. CMOS transceivers are being designed to deploy systems that offer the flexibility of high integration and low cost. The free-space wavelength ranges from 5 to 3.3 mm at these frequencies, which makes it difficult to design the radiators on the integrated circuit (IC) substrate. As a result most antennas are fabricated on an interposer or packaging substrate which does not suffer the losses of silicon. Antenna-in-package approaches to system integration utilize low loss dielectrics with low permittivity values. Planar antennas can be implemented in single or multilayer dielectric stacks common in laminate board manufacturing. Microfabrication methods can be applied to realize the printed radiators that have a low profile and low gain. While the antennas are not fabricated on the IC substrate they are still planar in nature and measured with ground-signal-ground (GSG) probes compared to being accessed using bulky coaxial-based connectors. At these frequencies, a custom designed measurement system may have to be developed to capture the antenna radiation pattern [2, 3]. Recently commercial systems

have been developed to facilitate accurate measurements using known system configurations. This paper presents the design, fabrication and performance of an aperture bowtie antenna printed on a planar laminate substrate. The bandwidth of the antenna is extended beyond the typical 30% by the use of sinusoidal modifications to the aperture [4]. The impedance bandwidth is measured from 50 to 110 GHz for 10 dB return loss (RL). The pattern bandwidth is calculated from measurements using the Nearfield Systems Inc. NSI-700S-360 spherical scanner. Principal pattern cuts will be shown from 60 to 85 GHz.

II. ANTENNA DESIGN AND FABRICATION

The modified aperture bowtie is defined to enhance the bandwidth by changing the input impedance using sinusoidal sections as detailed in [4] for a design operating in C band. It is based on the coplanar waveguide (CPW) fed planar aperture bowtie published by Zheng that radiates broadside [5]. The C band antenna was patterned on a copper metallized Rogers RT/Duroid substrate ($\epsilon_r = 2.2$, $\tan \delta = 0.0009$). The 0.017 mm metal layer was defined using a LPKF milling machine for a dielectric substrate height of 0.787 mm. The backside metal was completely removed to realize a uniplanar design using CPW feeds. The measured fractional bandwidth of the antenna was 54% centered at 6.4 GHz and the measured gain was 4.6 dBi at 5 GHz and 9.5 dBi at 7.5 GHz. The radiation patterns were obtained using a NSI 300V 6x6 planar near-field scanner.

The aperture antenna was initially developed for the purpose of designing a broadband radiator operating from 180 to 300 GHz for a silicon-based on-chip solution in a wide bandwidth system. When broadband antennas are implemented for multiband system operation, they reduce the number of required radiators. In an effort to understand the design considerations of the millimeter wave antenna, it was scaled down to 3 to 8 GHz where radiation pattern measurements could be obtained. From that point the design was frequency-scaled by a factor of 11.6 up to the 60 to 90 GHz range. For these frequencies, it was still easier to design antennas separate from the IC because they take up a large area and do not suffer from surface waves losses. In E-band, RL measurements were taken for impedance performance but it was not possible at that time, to measure the radiation pattern of the antennas. In 2015 we procured a NSI-700S-360 spherical near-field antenna

measurement system, which operates from 67 to 110 GHz using Oleson Microwave (OML) modules and an Agilent PNA for the RF subsystem. Due to its modular nature, the system can be scaled up further to cover the 180 to 300 GHz band using additional WR-5 and WR-3 modules.

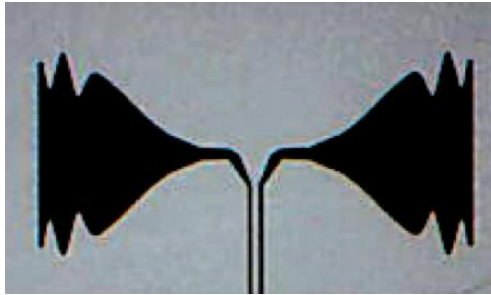


Figure 1. Modified aperture bowtie antenna.

The E band antenna is shown in Figure 1 and was fabricated in two ways. One antenna design was implemented in a single layer of FR408 (Isola Global) laminate ($\epsilon_r = 3.65$ and $\tan \delta = 0.018$) with a dielectric height of 0.125 mm and copper metallization of 0.012 mm. The CPW width and gap dimensions are 75 μm and 20 μm , respectively. This design was patterned using standard photolithography in a clean room with photoresist S1813. MG Chemicals ferric chloride was used to completely remove the backside metal and protect the antenna pattern on the front side of the substrate. The second design was manufactured by Ividen Corporation [6] and was realized in a multilayer stack-up using a FR-4 core. The core has improved thermal and mechanical properties compared to standard FR-4. The total height of the multilayer stack is 0.161 mm with 0.017 mm copper metallization. The overall antenna area is 6 mm x 3 mm, including the ground plane. Table 1 shows the material properties of the multilayer stack. The solder mask is listed as Layer 1 and is the lowest dielectric.

Table 1: Material properties of multilayer stack

Layer	ϵ_r	$\tan \delta$	Height/(mm) position
FR-4 core	4.8	0.015	0.060 / Layer 3
Build-up	3.3	0.018	0.054 / Layer 2, 0.037 / Layer 4
Solder mask	3.8	0.026	0.010 / Layer 1

III. MEASUREMENT SYSTEM

The antennas were measured in a near-field range using the NSI-700S-360 Spherical Near-field (SNF) Antenna Measurement System. The NSI-700S-360 is a new system designed to measure stationary mm-wave on-chip antennas. The NSI-700S-360 uses a multi-axis high accuracy stepper motor positioning system to move the probe on a spherical surface while the AUT remains stationary. The system incorporates RF converter modules from OML as part of the

probe carriage assembly and maintains a probe tip radius of roughly 20" (500 μm). Figure 2 shows the system installed in the UT Dallas measurement chamber.

The 700S-360 consists of a 500 mm positioner mounted vertically on a stable platform mounted to the floor. This positioner defines the horizontal ϕ -axis of rotation and coincides with the z-axis of the measurement coordinate system, as shown in Figure y. A second rotary stage is attached at an angle of 90° to the ϕ -axis and forms the θ -axis of a conventional right handed polar spherical coordinate system. A third rotary stage is attached to the θ -stage at an angle of 90° to the θ -axis and forms the χ -axis.

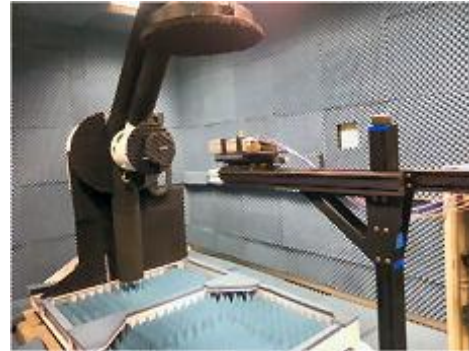


Figure 2. NSI-700S-360 in UT Dallas antenna chamber.

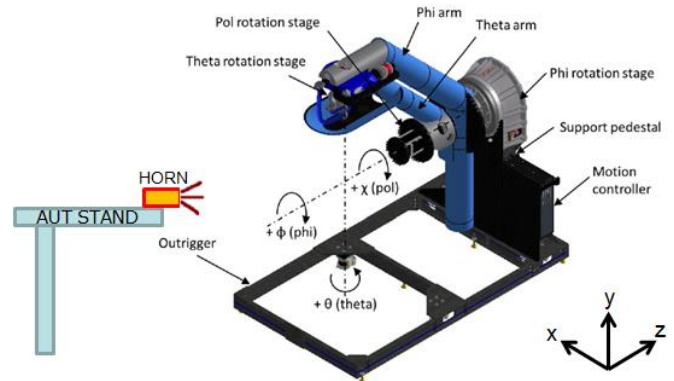


Figure 3. NSI-700S-360 coordinate system.

The combined motion of the ϕ and θ stages allows the probe tip to describe the trajectories located on a spherical surface centered about the intersection of the three orthogonal axes, whose definition is in accordance with standard SNF theory [7]. Similar to planar measurements, data is acquired across a two-dimensional sampling interval with the antenna under test (AUT) remaining stationary, which is desirable when measuring on-chip millimeter-wave antennas. The total range of motion is depicted in Figure 3 and spans a surface limited by $-110^\circ \leq \theta \leq 110^\circ$ and $0 \leq \phi \leq 180^\circ$. Those limitations are determined by the requirement to locate the RF rack and AUT support in the keep-out region as shown in Figure 2.

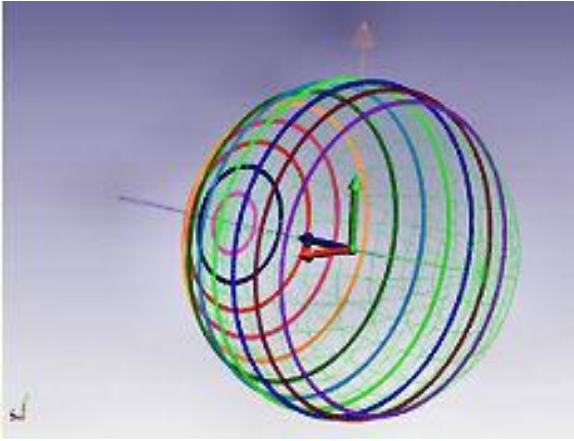


Figure 4. NSI-700S-360 scanner probe tip trajectory.

The axes shown in Figure 4 are: z-axis (blue, horizontal and pointing at N-pole), y-axis (green, vertical), x-axis (red, horizontal). The radial distance variation measured was ± 2.0 mm and angular location variation was $\pm 0.4^\circ$ peak-to-peak for both θ' and ϕ' . Based on the result of the measurement radius r' a corresponding electrical phase correction pattern may be generated at each frequency of interest. This phase correction can then be applied to the measured SNF data as a first order correction term in an attempt to remove the phase impact of the structural variation. Although a similar correction can be considered for angular uncertainties, these are typically found to be secondary in nature [8].

The mm-wave modules are exchangeable to cover the desired frequency bands, leaving the rack and cabling portion of the RF sub-system intact, making for a very modular and upgradable test system. The positioners contain integrated RF rotary joints to maximize cable phase stability during testing and the Phi-axis positioner also contains a slip-ring assembly. The measurement system includes an adjustable AUT stand, which provides a stable base for the AUT platform, positioners and the millimeter wave module. Figure 5 shows the UT Dallas AUT probing platform mounted on the AUT stand.



Figure 5. UT Dallas AUT probe platform with orientation of planar antenna.

IV. MEASUREMENTS VS. SIMULATION

A. Return Loss

The antennas were measured on a Cascade Microtech M150 probe station from 50 to 110 GHz using a 100 μm pitch GGB ground-signal-ground (GSG) Picoprobe. The antennas

were placed on a 6" piece of Rohacell® 51 HF ($\epsilon_r = 1.04$, $\tan \delta = 0.0135$ at 26.5 GHz) closed cell foam, manufactured by Evonik Industries. A short-open-load (SOL) calibration was performed up to the probe tip using a CS-5 impedance standard substrate (ISS).

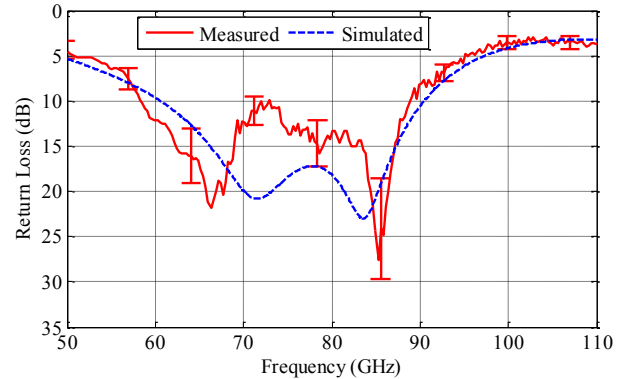


Figure 6. Measured versus simulated RL of aperture bowtie fabricated on FR408 [5].

The RL magnitude is shown in Figure 6 for the antenna manufactured on FR408. The measured 10 dB bandwidth (BW) ranged from 58 to 88 GHz, which corresponds to a fractional BW of 41% centered at 73.6 GHz. Although not shown, the antenna fabricated by Iridium had similar performance with a 10 dB BW ranging from 58 to 92 GHz, which corresponds to a fractional BW of 45%.

B. Radiation Patterns

The simulated broadside gain for the FR408 antennas is shown in Figures 7 and 8. The gain is 6.38 dBi at 65 GHz and 5.42 dBi at 85 GHz. The E-plane (solid red curves) cut has minima at 90° and 270° , with maxima at 0° and 180° , for both frequencies. The simulated 3 dB beam width of the H-plane (dashed blue curves) at both frequencies is narrower than the E-plane. At 85 GHz the simulated H plane pattern introduces nulls at $\pm 30^\circ$ because the antenna's length is comparable to λ at that frequency.

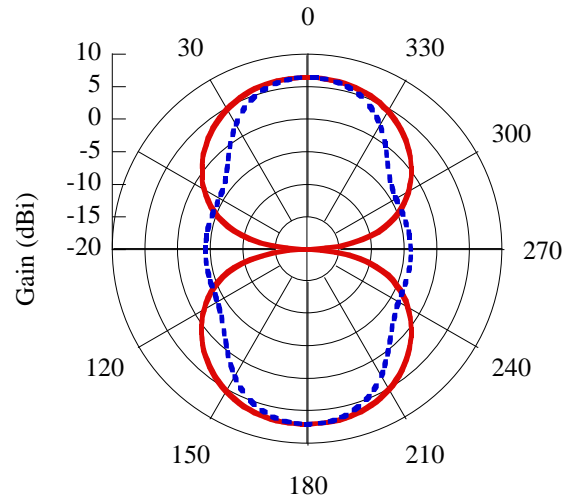


Figure 7. Simulated FR408 radiation patterns at 65 GHz [5].

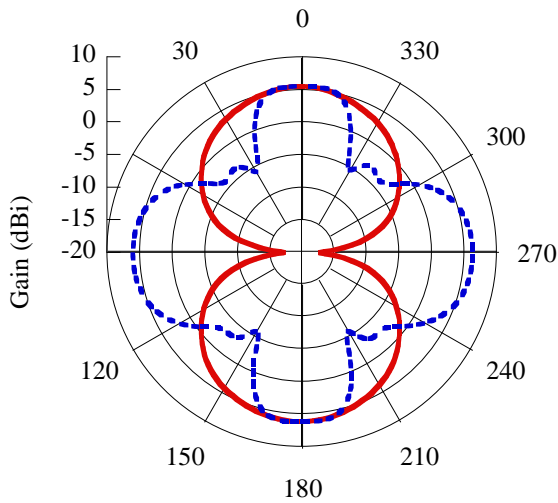


Figure 8. Simulated FR408 radiation patterns at 85 GHz [5].

The fabricated antennas were mounted on the AUT probe platform in Figure 5 using double-sided tape. The antenna is supported by ten layers of Rohacell® 71 HF ($\epsilon_r = 1.093$, $\tan \delta = 0.0155$ at 26.5 GHz). A single layer that is 6.25 mm thick is combined using adhesive to realize a total height of 62.5 mm. The material rests firmly in the AUT stand with an additional step height to accommodate the probe positioner z-axis travel. Absorber material is placed across the top of the platform to shield the frequency module and probe manipulator. For the FR408 sample, a multi-frequency near-field scan was taken using NSI 2000 software and the GGB Picoprobe. Measured radiation patterns show results similar to simulation with the NSI-700S-360 in Figures 9 and 10.

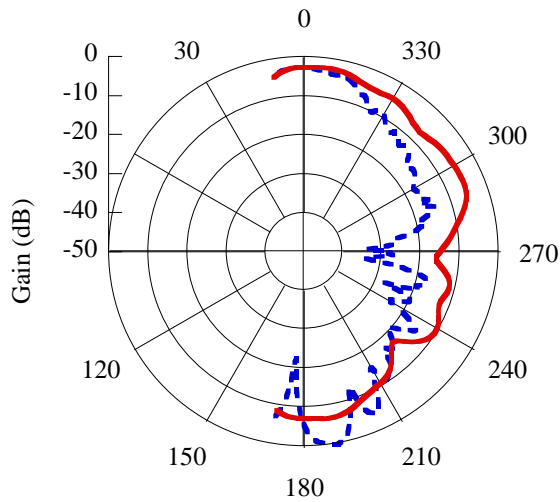


Figure 9. Measured FR408 radiation patterns at 70 GHz.

The low frequency measurements were taken at 70 GHz since the NSI system starts at 67 GHz (OML module design). Due to the location of the AUT stand, the radiation pattern is shown from -10° to $+170^\circ$. At 70 and 85 GHz, the E-plane cut (solid red curves) has a minimum at -90° that is 16 dB below the

maxima at 0° . The H-plane (dashed blue curves) is narrower than the E-plane cut at 70 GHz, although it widens at 85 GHz. At 85 GHz, a dip is observed at 20° in the H-plane in simulation and measurement. The null in the H-plane can be attributed to reflections caused by the probe body itself and the Cascade mount, however the Cascade positioner and AUT stand are also contributors.

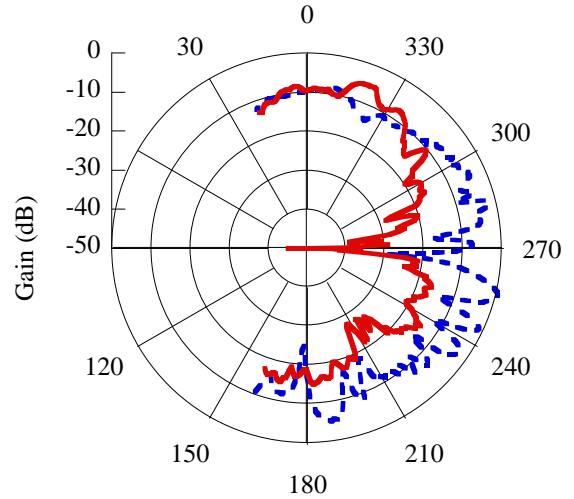


Figure 10. Measured FR408 radiation patterns at 85 GHz.

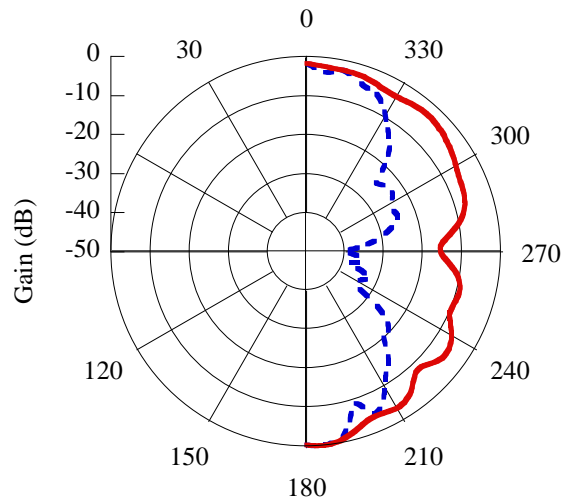


Figure 11. Measured Iridium multilayer antenna radiation patterns at 69 GHz.

A single frequency measurement of the principle planes for the Iridium structure is shown in Figure 11. This antenna was measured using a $150 \mu\text{m}$ pitch probe manufactured by MPI Corporation. The pattern is similar to the 70 GHz FR408 antenna with the E-plane (solid red curve) having a 13 dB null at -90° . It is believed that the layered Rohacell structure and adhesive used to support the AUT may have an impact on all the radiation patterns in the lower half plane causing the ripples in the responses compared to simulation.

V. SUMMARY OF RESULTS

This paper presented the design, fabrication and characterization of a CPW-fed modified aperture bowtie antenna fabricated using laminate substrates for operation in the 60-90 GHz range. The radiation patterns of these antennas were measured in the NSI-700S-360 and show good agreement to electromagnetic simulation.

ACKNOWLEDGEMENT

The authors would like to thank the Evonik Industries for the Rohacell® samples, Isola Global for the FR408 material, and the UT Dallas cleanroom and Texas Instruments for assistance in fabrication. This work was partially supported by Semiconductor Research Corporation (SRC) Task #1836.122 through the Texas Analog Center of Excellence (TxACE) and by the Office of Naval Research (ONR) Defense University Research Instrumentation Program (DURIP).

REFERENCES

- [1] D. Liu, B. Gaucher, U. Pfeiffer, J. Grzyb, *Advanced millimeter-wave technologies, antennas, packaging and circuits*, Wiley, 2009, United Kingdom.
- [2] K. V. Caekenberghe, et al., "A 2-40 GHz probe station based setup for on-wafer antenna measurements," *IEEE Trans. on Antennas & Propagation*, vol. 56, no. 10, pp. 3241-3247, 2008.
- [3] S. Beer, T. Zwick, "Probe based radiation pattern measurements for highly integrated millimeter-wave antennas," 2010 Proceedings of the Fourth European Conference on Antennas & Propagation, pp. 1-5.
- [4] R. G. Pierce, A. J. Blanchard, R. M. Henderson, "Broadband planar modified aperture bowtie antenna," *IEEE Antennas and Wireless Propagation Letters*, vol. 12, pp. 1432-1435, 2013.
- [5] R. Pierce, "Broadband planar millimeter wave radiators," Ph.D. dissertation, Dept. Elect. Eng., The University of Texas at Dallas, 2014.
- [6] G. Zheng, A. Z. Elsherbeni, C. E. Smith, "A coplanar waveguide bowtie aperture antenna," *IEEE Antennas & Propagation Society International Symposium*, 2002.
- [7] S. Aroor, "System-on-package integration for millimeter-wave circuits using low-cost laminates," Ph.D. dissertation, Dept. Elect. Eng., The University of Texas at Dallas, 2013.
- [8] C. Parini, S. Gregson, J. McCormick & D. Janse van Rensburg, *Theory and Practice of Modern Antenna Range Measurements*, IET, London, 2014. ISBN 978-1-84919-560-7.
- [9] D. Janse van Rensburg, *Factors Limiting the Upper Frequency of mm-Wave Spherical Near-field Test Systems*, EuCap 2015, Lisbon, Portugal, April 2015.